TITLE: Three-dimensional culture in a bioengineered matrix and somatic cell complementation to improve growth and survival of bovine preantral follicles

Juliana I. Candelaria[1], Ramon C. Botigelli[1], Carly Guiltinan[1], Ariella Shikanov[2,3,4], Anna C. Denicol[1*]

[1]Department of Animal Science, University of California Davis, Davis, CA, USA.

[2] Department of Biomedical Engineering, University of Michigan, Ann Arbor, MI, USA.

[3]Department of Obstetrics and Gynecology, University of Michigan, Ann Arbor, MI, USA.

[4]Department of Macromolecular Science and Engineering, University of Michigan, Ann Arbor, MI, USA.

*Corresponding author: Anna C. Denicol

acdenicol@ucdavis.edu

STRUCTURED ABSTRACT

Purpose: Novel assisted reproductive technologies that capitalize on the preantral follicle population and utilize stem cell biology are greatly warranted. In this study, we explored the use of poly(ethylene glycol) (PEG) bioengineered hydrogels for bovine preantral follicle culture with or without ovarian cell co-culture, and examined the propensity of bovine embryonic stem cells (bESCs) to differentiate towards gonadal somatic cells. Together, these technological advances can be complemented to develop a sustainable and dynamic follicle culture system similar to the ovarian microenvironment.

Methods: Bovine preantral follicles at the primary and early secondary stages were cultured in two-dimensional (2D) control or encapsulated in PEG hydrogels (3D) to assess growth and then co-cultured in PEG hydrogels with bovine ovarian cells (BOCs) to determine cell and follicle viability. In a separate experiment, we tested protocols to modulate WNT, FGF and BMP4 signaling to drive differentiation of bESCs towards the

intermediate mesoderm and bipotential gonad-like fate and measured gene and protein expression of key lineage markers.

Results: Primary follicles (40-60 µm), but not early secondary follicles (61-70 µm), grew over the 10-day culture period in PEG hydrogels compared to 2D control. However, follicles co-encapsulated with BOCs in hydrogels did not maintain viability and BOCs lost stromal cell signature over the culture period. When bESCs were induced towards gonadal somatic cells under WNT signaling activation, bFGF and BMP4 were dispensable to upregulate intermediate mesoderm (*LHX1*) and early coelomic epithelium/bipotential gonad markers (*OSR1*, *GATA4*, *WT1*). Higher BMP4 concentrations upregulated the lateral plate mesoderm marker *FOXF1*. Expression of *PAX3* did not change over the course of the culture, indicating that the paraxial mesoderm lineage was not induced.

Conclusions: Culture of preantral follicles at the primary stage in PEG hydrogels resulted in follicle growth compared to 2D system, although the benefit of the 3D system was inconsistent. BOCs did not maintain their identity in the PEG hydrogels; collectively, these results demonstrate that the PEG hydrogels can be a potential culture system for early stage follicles after refinements are implemented. These refinements could include the addition of ESC-derived ovarian somatic cells using protocols such as the one described here.

KEYWORDS

Preantral follicle, three-dimensional culture, embryonic stem cells, ovary, bovine, biomimetic

53 CAPSULE SUMMARY
54
55 We demonstrate that three-dimensional bioengineered hydrogels could aid in the survival
56 and growth of small bovine preantral follicles. Moreover, bovine embryonic stem cells
57 have the potential to differentiate towards precursors of somatic gonadal cell types,
58 presenting an alternative cell source for preantral follicle co-culture.

INTRODUCTION

Folliculogenesis is a complex and selective process resulting in production of a limited quantity of meiotically and developmentally competent oocytes over a female's lifespan. The molecular processes that coordinate the activation, growth and maturation of ovarian follicles have yet to be fully elucidated, especially during the early preantral stages of development. Progress in understanding preantral folliculogenesis in non-rodent species has been hindered by the lack of appropriate in vitro culture systems and an insufficient knowledge base of ovarian development and function. This is particularly true in large mammal (i.e. cows and humans) preantral folliculogenesis which have prolonged duration and sizeable volumetric changes between the primordial and pre-ovulatory follicle stages. A great advantage of performing in vitro folliculogenesis beginning at the preantral stage includes establishing an alternative fertility preservation and restoration method by utilizing the vast preantral follicle pool for oocyte production [1]. More specifically, this approach would be beneficial for prepubertal girls suffering from blood-borne malignancies as isolated preantral follicles could be matured in vitro without the risk of reintroducing malignant cells or surgical intervention, as could be the case with the culture and reintroduction of ovarian tissue fragments.

Recapitulation of bovine preantral folliculogenesis has been attempted by several groups, but there has been little success in efficiently growing follicles to the preovulatory stage and yielding metaphase II oocytes. Although 2-dimensional culture systems have shown some promise in supporting bovine preantral follicle growth [2–4], mounting evidence suggests that 3-dimensional (3D) culture systems better promote development due to their ability to maintain a follicle's spherical configuration and preserve cell contact

82 both within the follicular unit (i.e. granulosa cell and oocyte interface) and outside the
83 basement membrane where theca cells are located [5–8]. Matrigel and alginate are
84 commonly used biomaterials to create hydrogels for in vitro follicle culture, however
85 pitfalls include uncontrollable degradation and biological inertness, respectively [9].
86 Therefore, a highlighted alternative is the use of bioengineered 3D hydrogel culture
87 systems that permit timely degradation by the follicle yet retaining the mechanical support
88 necessary to keep its spherical structure [10,11]. Poly(ethylene glycol) (PEG) hydrogels
89 constructed with proteolytically-degradable peptide crosslinkers have been employed for
90 mouse in vitro folliculogenesis and demonstrated success in growing preantral follicles to
91 the antral stage and producing metaphase II oocytes [12]. Likewise, the addition of
92 adipose-derived stem cells or conditioned media to PEG hydrogels containing mouse
93 preantral follicles further aided development and survival [13]. Despite the promise
94 demonstrated in mice, the use of PEG hydrogels for large mammal in vitro preantral
95 follicle culture has not been reported. Moreover, investigating cell supplementation in the
96 hydrogel system to determine their propensity to become theca cells and/or
97 advantageous effect on follicle growth has not been directly assessed. Indeed, early
98 preantral follicles do not contain theca cells and must recruit precursor cells from the
99 stromal environment to build the essential theca layer, hence addition of cells to the
100 system would be essential when starting with primordial- or primary-stage follicles. More
101 specifically, the hedgehog signaling pathway is key to driving theca cell differentiation and
102 recruitment [14–16], therefore cells added to the culture system should harbor the cellular
103 machinery to respond to hedgehog ligands secreted by the follicular granulosa cells.

104 Although native ovarian stromal cells have been used as feeder cells for 2D and
105 3D in vitro follicle culture [17–19], surgical intervention is required to obtain ovarian tissue
106 and harvest cells. Moreover, their abilities to phenotypically-mirror theca cells upon co-
107 culture with follicles has not been shown to date. Alternative cell sources, particularly
108 those of renewable capacity (i.e. stem cells) present a unique advantage to generating
109 cells that could give rise to a theca cell-like phenotype. To that end, stepwise in vitro
110 differentiation of pluripotent stem cells into gonadal-like cells has been demonstrated in
111 humans and mice [20–22] thus highlighting the potential to create a substitute cell source
112 with prospective theca cell characteristics. Cell fate decisions that result in formation of
113 the bipotential gonad in the embryo are the culmination of precisely timed cell signaling
114 via gradients of morphogens such as FGF, BMP, and WNT proteins. Hence, protocols
115 have been devised employing a stepwise induction of pluripotent stem cells using FGF,
116 BMP, and WNT signaling such that cells progress through a mesoderm-like state, and
117 finally a bipotential gonad-like state [23–25].

118 In this study, we describe the use of a PEG hydrogel culture system with or without
119 native ovarian cells for the in vitro development of bovine preantral follicles and explore
120 the potential of bovine embryonic stem cells to be induced towards gonadal-like cells in
121 vitro. We first hypothesized that culture in PEG hydrogels would improve the growth and
122 viability of bovine preantral follicles. By examining the gene expression of ECM-degrading
123 enzymes of primary- and early secondary-stage follicles, we tailored the hydrogel design
124 to respond to bovine follicle enzyme secretion. Based on the evidence that cell
125 supplementation improves mouse follicle development, we also examined the effect of
126 dissociated bovine ovarian cells (BOCs) on bovine preantral follicle growth and if BOCs

127 exhibit a pre-theca cell phenotype when cultured in vitro using PEG hydrogels. Finally,
128 we hypothesized that bovine embryonic stem cells (bESCs) can be differentiated into the
129 intermediate mesoderm and early coelomic epithelium/bipotential gonad.
130

131 MATERIAL AND METHODS
132
133 All materials were purchased from Thermo Fisher Scientific unless otherwise specified.

134 *Follicle Isolation and bovine ovary single-cell dissociation*

135 Fresh bovine preantral follicles were isolated as previously described [26]. Follicles
136 were maintained in warmed follicle wash media until subsequent experiments. For bovine
137 ovary single-cell dissociation (n = 3 replicates), cortical tissue (250-300 mg) was
138 fragmented into 500 μm^2 pieces incubated with Hank's balanced salt solution (Ca^{2+}/Mg^{2+})
139 containing 1 mg/mL collagenase IV, 1 U/mL DNase I, and 50 µg/mL Liberase
140 (5401119001, Sigma Aldrich). The solution with tissue was shaken at 38.5 °C for 20 min,
141 pipetted 15 times using a serological pipette, and shaken again for 20 min to mechanically
142 aid in the dissociation of cells. Enzymatic activity was stopped by adding 20% v/v fetal
143 bovine serum to the solution. The tissue-dissociated solution was filtered through a 100
144 µm then through a 35 µm cell strainer. Cells collected after final filtration were centrifuged
145 (300 x*g* for 5 min) and the resulting pellet was resuspended in 1 mL Hank's balanced salt
146 solution without Ca^{2+}/Mg^{+} until encapsulation.
147

148 *PEG hydrogel materials, preparation, and follicle encapsulation*

149 PEG hydrogel experiments were conducted using 8-arm PEG vinyl sulfone (PEG-
150 VS) (40 kDa, >99% purity, JenKem Technology) and crosslinked with MMP- and Plasmin-

151 sensitive peptide sequences (Ac-GCRD**VPMS**MRGGDRCG**YKNS**CG, i.e. YKNS/VPMS)
152 (2391.8 g/mol, >90%, Celtek Peptides). PEG and crosslinker peptide were dissolved in
153 isotonic 50 mM HEPES buffer and mixed to a final composition containing 5% PEG-VS
154 with 1:1 stoichiometric ratio of VS to thiol (side chain present on cysteines in peptide
155 sequence). Sixteen-µl hydrogels containing preantral follicles were formed between
156 parafilm-lined glass slides and allowed to gelatinize for up to 10 min. Then, hydrogels
157 were transferred to warmed follicle maintenance media to swell and placed in a humidified
158 incubator (37°C). Freshly isolated follicles were maintained in warmed follicle wash media
159 until encapsulation. In experiment 1, follicles (n = 1-4) were first washed in 10% PEG-VS
160 and either encapsulated in PEG hydrogels or placed into 2D culture. Hydrogel-
161 encapsulated and 2D culture follicles were placed into individual wells of a 96-well plate
162 containing follicle culture media (1:1 ratio of α-MEM and F12 with glutamine
163 supplemented with 3 mg/mL bovine serum albumin, 100 ng/mL penicillin/streptomycin,
164 1 mM sodium pyruvate, 1 % (v/v) non-essential amino acids, 10 mg/l insulin, 5.5 mg/l
165 transferrin and 6.7 µg/L selenium (ITS), 100 ng/mL human recombinant follicle stimulating
166 hormone (228-12609-2, RayBiotech), and 50 µg/mL ascorbic acid. Half of the spent media
167 was changed every 2 days and follicles were cultured for 10 days. To assess follicle
168 growth over the culture period, the average of 2 perpendicular diameter measurements
169 were taken at day 0, day 5, and day 10 using an inverted microscope (Revolve, Echo
170 Labs). The percentage of growing and non-growing follicles (growth defined as having at
171 least 5% increase in diameter by day 10 compared to day 0) and percent increase in size
172 in growing-only follicles was calculated. In total, 15 replicates were conducted with a total
173 of 216 follicles (n = 153 in PEG and n = 63 in 2D control)

174 *Cell viability staining and quantification*

175 Bovine ovarian cells and MeLCs were resuspended in PEG-VS + crosslinker
176 peptide VPMS/YKNS at a concentration of 1, 2, 10, and 20 x 10^6 cells/mL to test cell
177 viability immediately after encapsulation, 5 and 10 days after in vitro culture. Hydrogels
178 were cultured individually in 96-well plates with 150 µl of follicle culture media with half
179 media changes every 2 days. After culture, hydrogels were incubated for 10 min with pre-
180 equilibrated alpha-MEM containing 2 µM propidium iodide (PI) and 1:1000 Hoechst (1
181 µg/mL final concentration). Negative control hydrogels were void of propidium iodide and
182 used for setting exposure limit during imaging. Hydrogels were imaged using an
183 epifluorescent microscope (Revolve) and the total number of cells and number of viable
184 cells were quantified using ImageJ after converting to binary images where PI/Hoechst-
185 positive cells were white, and background was black. Total number of cells positive for PI
186 were divided by total cells quantified by Hoechst staining to determine percentage of
187 unviable cells. Percentage of viable cells was determined by subtracting percentage of
188 unviable cells from 100. The experiment was repeated 4 times using 3 hydrogels per cell
189 density for each replicate.

190

191 *Bovine ovarian cells with follicle encapsulation and culture in PEG*

192 To test the impact of BOC and co-encapsulation on follicle viability and growth and
193 theca cell differentiation during in vitro culture, hydrogels were formed with either 1) only
194 follicles, 2) 5 x 10^6 BOCs/mL only, or 3) follicles and 5 x 10^6 BOCs/mL BOCs. Each
195 hydrogel contained 1-5 follicles (n = 65 follicles); 5 replicates). Hydrogel formation and
196 follicle encapsulation was performed as previously described with the addition of staining

197 follicles with the cell membrane marker PKH26 (2 μM final concentration; Sigma-Aldrich)
198 prior to encapsulation to improve visualization. Hydrogels were cultured for 10 days with
199 half of the medium changed every other day. Follicles were considered viable if the
200 basement membrane was attached, the follicles were void of vacuoles, and granulosa
201 cells were not darkened or mishappened. To recover cells for RT-qPCR, the hydrogels
202 were incubated in phenol red-free alpha-MEM with Liberase (1.3 wünsch units/mL) and
203 incubated at 37 °C and 5% CO_2 for 30 min with repeated pipetting to degrade the hydrogel
204 and extract the cells. After centrifugation, the cell pellet was used for RNA extraction,
205 cDNA synthesis and RT-qPCR as described below.
206
207 *Culture of bovine embryonic stem cells (bESCs)*
208 Bovine embryonic stem cells (n = 2 female lines) were routinely cultured feeder-
209 free in NBFR medium (N2B27 medium [1:1 DMEM/F12 and Neurobasal media, 0.5% v/v
210 N-2 supplement, 1% v/v B-27 supplement, 2 mM MEM Non-Essential Amino Acid
211 solution, 1% v/v GlutaMAX supplement, 0.1 mM 2-mercaptoethanol, 100 U/mL Penicillin,
212 and 100 μg/mL Streptomycin] supplemented with 1% bovine serum albumin (BSA), 20
213 ng/mL bFGF (100-18B, PeproTech), 2.5 μM IWR-1 (I0161, Sigma), and 20 ng/mL Activin
214 A (338-AC, R&D Systems)]. Cells were passaged onto vitronectin-coated plates every 2-
215 4 days using TrypleExpress at 1:4-1:6 split ratio and cultured in humidified incubators at
216 37 ºC and 5% CO_2. When cells were passaged, media was supplemented with 10 μm
217 ROCK inhibitor Y-27632. Media was changed daily and bESCs used for mesoderm
218 induction were between passage 18-26.

219 For mesoderm induction, bESCs were passaged onto 12-well vitronectin-coated
220 plates at 40,000 cells per well in mesoderm-induction media [GMEM medium, 15%
221 knockout serum replacement, 0.1 mM NEAA, 2mM GlutaMAX, 1mM sodium pyruvate,
222 0.1mM β-mercaptoethanol , 100 U/mL Penicillin, and 100 µg/mL streptomycin and
223 supplemented with 3 µm CHIR99021 and 70 ng/mL Activin A]. Cells were cultured in
224 mesoderm induction medium for 48 hours with daily medium change and thereafter the
225 cells were considered "mesoderm-like cells" (MeLCs) and used for subsequent
226 experiments.

227 Mesoderm-like cells were cultured in mesoderm induction medium without activin
228 A for an additional 72 hours and supplemented with 10 ng/mL bFGF beginning
229 immediately after MeLC induction, 24 hours after MeLC induction, 48 hours after MeLC
230 induction, or no supplementation (mesoderm medium only). Based on the finding of which
231 bFGF regimen best upregulated gene expression, in a second experiment, MeLCs were
232 cultured in mesoderm induction media without activin A, with 10 ng/mL bFGF and with
233 either 0, 1, 10, or 20 ng/mL of BMP4 for an additional 72 hours. All experiments contained
234 duplicate wells for each condition tested and had 3 biological replicates/independent
235 differentiations. Cells were imaged every day during each differentiation on the EVOS
236 (Thermo Fisher) inverted microscope.

237

238 *End-point (RT-PCR) and quantitative reverse transcription PCR (qRT-PCR)*

239 Freshly isolated follicles were pooled by stage and snap frozen in minimal PBS. To
240 examine the expression of transcripts for extracellular-matrix degrading enzymes,
241 primary follicles (n = 3 pools of 46-56 follicles per pool) and early secondary follicles (n =

242 3 pools of 34-40 follicles per pool) were subjected to RNA isolation using a protocol with
243 a combination of Trizol, Purelink DNase treatment, and Qiagen RNeasy Micro Kit. Final
244 total RNA was eluted into 14 µl of RNase-free water. Bovine ovarian cells (BOCs), bESCs,
245 MeLCs and differentiated cells were pelleted, snap frozen, and subjected to RNA isolation
246 following manual instructions using the Qiagen RNeasy Micro Kit. Maximum available
247 RNA mass was used for cDNA synthesis of primary and early secondary follicles and 250
248 ng - 1 µg of total RNA was used for cDNA synthesis of bESCs, BOCs, MeLCs, and
249 differentiated cells (RevertAid cDNA Reverse Transcription Kit). For RT-qPCR, 1-2 µl of
250 cDNA (50 ng total), 1x SsoAdvanced Universal SYBR Green Supermix (Bio-Rad,
251 Hercules, CA), and 250 nM of forward and reverse primers were mixed for 10 µl total
252 volume and pipetted into 96-well plates. The reaction was carried out in the CFX96 Touch
253 Deep Well Real-Time PCR Detection System (Bio-Rad). Cycling conditions were an initial
254 denaturation step at 95 ºC for 30 sec followed by 40 cycles of denaturation at 95 ºC for
255 10 sec, annealing at 60 ºC for 30 sec, and extension at 60 ºC for 5 sec. To confirm
256 specificity of PCR products for each gene, each assay included a melt curve analysis and
257 non-template control. Data was normalized to *ACTB* by the delta-Ct method and relative
258 expression data are represented as 1/ΔCT. For conventional PCR, PCR products from
259 quantitative PCR reactions were ran on a 2% agarose gel to visualize the PCR products.
260 For RT-qPCR experiments using *BAX* and *BCL2* primers, a standard curve of fresh
261 bovine ovarian cells was used to estimate absolute quantity of mRNA present in unknown
262 samples of BOCs. The ratio of *BAX*/*BCL2* was calculated from mRNA quantity of
263 respective genes and used to determine if cells were in a pro- or anti-apoptotic state. All
264 primers used in these experiments are listed in Table 1.

265 *Statistical analysis*

266 All data was first assessed for normality using a Shapiro-Wilk test. PEG growth
267 data was subjected to a two-way ANOVA using RStudio with effect of replicate included
268 in the model. Cell viability and RT-qPCR data were subjected to a one-way ANOVA or
269 Kruskal-Wallis test if data was not normally distributed using Graph Prism. Post-hoc tests
270 (Tukey's and Dunn's for ANOVA and Kruskal-Wallis, respectively) were conducted when
271 appropriate. RT-qPCR data were analyzed based on delta-Ct values. Comparisons were
272 considered significantly different when associated with $P < 0.05$.

273

274 RESULTS

275 To design a proteolytically-degradable PEG hydrogel that would most likely be
276 compatible with bovine preantral follicles, we first examined the gene expression of ECM-
277 degrading enzymes in primary and early secondary follicles that express the key follicle
278 marker *FSHR*. Matrix metalloproteinases (MMPs) and plasminogen activators are ECM-
279 degrading enzymes and play a pivotal role in tissue remodeling. We found the bovine
280 primary and early secondary follicles express *MMP2*, although in one pool we only found
281 *MMP2* in early secondary follicles. However, neither follicle stage expressed *MMP9*
282 (Figure 1A). Plasminogen-activator urokinase (*PLAU*) was expressed in primary and early
283 secondary follicles from one pool, but not in the second or third pool. Similarly,
284 Plasminogen-activator tissue (*PLAT*) was expressed in primary follicles of one pool and
285 in early secondary follicles from two other pools (Figure 1A). Since we collectively found
286 mRNA expression of *MMP2* and plasminogen enzymes, we proceeded with using a PEG

287 hydrogel that is functionalized with VPMS (MMP-sensitive) and YKNS (plasminogen-
288 sensitive) peptide sequences (Figure 1B).

289 Next, we tested the hypothesis that bovine preantral follicles are more likely to
290 grow and demonstrate greater growth rate when encapsulated in PEG hydrogels
291 compared to 2D traditional methods after 10 days of culture. We found no difference in
292 the percentage of growing follicles between PEG (35.8% ± 6.23%) and 2D control (30.3%
293 ± 7.88%) (P = 0.56) (Figure 2A). We found that replicate (i.e. individual ovary) affected
294 the percentage of growing follicles (P < 0.05) regardless of culture condition. It is worth
295 noting that in the control group, no follicle growth was observed in four out of the 15
296 replicates, whereas in the PEG group there was growth, although variable, in every
297 replicate (Figure 1A). Of the replicates where at least one follicle demonstrated growth in
298 either condition, we found no difference (P = 0.50) in the growth rate from initial size (PEG:
299 18.8% ± 3.32%, control: 22.7% ± 3.49%) (Figure 2B). There was no effect of replicate on
300 growth rate (P = 0.78).

301 We further examined the diameter changes between day 0, 5, and 10 in follicles
302 within a narrow range of starting diameters corresponding to their stage of development
303 between the primary to early secondary. When we examined follicles with starting
304 diameters corresponding to the early primary stage (40-60 μm), we found PEG hydrogels
305 outperformed the control conditions as day 5 follicles were larger in PEG compared to 2D
306 control (P < 0.05). Moreover, by day 10, PEG hydrogel follicles had a significant increase
307 in diameter compared to day 0 (P < 0.05), whereas control follicles showed no difference
308 (P = 0.72). Follicles starting at 61-70 μm showed a decrease in diameter by day 10 of
309 culture in control conditions (P < 0.05), whereas follicles cultured in PEG maintained a

310 similar diameter over time (P = 0.68; Figure 2C). Therefore, day 5 and 10 follicles were
311 significantly smaller (P < 0.05) in control follicles when compared to similar timepoints of
312 PEG follicles. A representative image of a follicle grown in a PEG hydrogel over the 10-
313 day period is depicted in Fig. 2D.

314 We evaluated cell viability of BOCs when encapsulated in PEG hydrogels and
315 cultured for 10 days (Figure 3A-C). When encapsulated at 1 or 2 x 10^6 cells/mL, BOCs
316 showed low cell viability (data not shown), whereas concentrations of 10 or 20 x 10^6
317 cells/mL showed high viability (70-90%) and cell aggregation (Figure 3B and C). In this
318 experiment, we found that neither control (no BOCs encapsulated) or hydrogels with
319 BOCs supported follicle growth over the 10 day-culture period (Figure 3D). Moreover,
320 gene expression analysis of pre-theca cell markers in the BOCs after 10 days of culture
321 revealed a decrease in expression of *PTCH1* (P < 0.01) and *GLI1* (P < 0.01) when
322 compared to day 0 fresh cells in both BOCs cultured alone and co-encapsulated with
323 follicles (Figure 3E). We found a decrease in both *BAX* and *BCL2* in BOCs that were
324 cultured with follicles and a decrease in *BCL2* in BOCs cultured in PEG hydrogels alone
325 (P < 0.05; Figure 3F). However, there was no difference in *BAX*/*BCL2* ratio, thus indicating
326 no difference in the pro- versus anti-apoptotic balance between cultured and fresh BOCs.

327 Given that native BOCs did not show maintenance of pre-theca identity or
328 contribute to follicle growth, we then explored the differentiation of bESCs into progenitor
329 cells of the bipotential gonad by testing effect of WNT, bFGF and BMP4 signaling (Figure
330 4A). We first tested the hypothesis that MeLCs exposed to a pulse of bFGF during
331 intermediate mesoderm/bipotential gonad differentiation would upregulate gene
332 expression of key markers at the end of induction (Figure 4B and C). Compared to bESCs

333 and 0, 24, 48, and 72 hours of 10 ng/mL bFGF exposure, MeLCs had higher expression
334 of the early lateral plate/intermediate mesoderm marker *LHX1* (Figure 4B; $P < 0.001$). We
335 also found the intermediate mesoderm marker *OSR1* to be upregulated in all bFGF
336 regimens compared to bESCs ($P < 0.01$). When analyzing expression of bipotential gonad
337 markers, there was no difference in *GATA4* ($P = 0.15$) across all experimental groups. We
338 also found higher expression of *WT1* after 0, 24, 48, and 96 hours of bFGF compared to
339 bESCs and MeLCs ($P < 0.001$). There was no difference in expression of *WT1* between
340 bESCs and MeLCs ($P = 0.15$). There was also no difference in expression of the paraxial
341 mesoderm marker *PAX3* across all experimental groups ($P = 0.06$), indicating induction
342 conditions did not show strong propensity to drive cells to the paraxial mesoderm fate.
343 However, the lateral plate mesoderm marker *FOXF1* was significantly upregulated
344 compared to bESCs in 0, 24, and 48 hours of bFGF exposure ($P < 0.05$).

345 Because all bFGF regimens tested caused elevation in *WT1* and *OSR1*
346 expression, we chose to use a 24-hour pulse of bFGF in the next experiments when
347 testing the synergistic effects of including various concentrations of BMP4 over the same
348 culture period time and in two bESC lines (Figure 5A, B, and C). Similar to the bFGF
349 experiment, we found the highest level of *LHX1* expression in MeLCs (Figure 5A; $P <$
350 0.0001). However, 10 and 20 ng/mL of BMP4 led to lower expression when compared to
351 bESCs ($P < 0.05$). Also confirming the previous results, *OSR1* was elevated in all
352 experimental groups, including MeLCs, when compared to bESCs ($P < 0.01$). Unlike in
353 the bFGF experiment where there was no difference amongst exposure times to bFGF,
354 we found an increase in *GATA4* in MeLCs and when 1, 10 or 20 ng/mL of BMP4 were
355 present ($P < 0.05$). *WT1* was upregulated in 0, 1, 10, or 20 ng/mL BMP4, but not in MeLCs

356 ($P < 0.05$). Again, we found no difference in *PAX3* expression among all concentrations
357 of BMP4 when compared to bESCs. As expected, increasing the concentration of BMP4
358 led to a significant increase in *FOXF1* ($P < 0.05$), indicating a likely shift towards the lateral
359 plate mesoderm lineage with rising levels of BMP4 which is similar to in vivo development.
360 We further assessed WT1 and OCT4 expression in bESCs, MeLCs, and cells
361 cultured with 0 and 1 ng/mL BMP4 as these concentrations led to elevated *WT1* without
362 greatly upregulating *FOXF1* (Figure 5B). We found positive nuclear staining for OCT4 in
363 bESCs and MeLCs and no signal in cells exposed to BMP4, indicating likely loss of
364 pluripotency after mesoderm induction. We found nuclear localization of WT1 in bESCs
365 and nuclear and cytoplasmic localization in MeLCs (48 h culture) and 0 ng/mL BMP4 (120
366 h culture). Interestingly, we did not observe WT1 expression at the protein level when
367 cells were exposed to 1 ng/mL BMP4.
368
369 DISCUSSION
370 To our knowledge, this study is the first to utilize a novel bioengineered PEG
371 hydrogel system for in vitro culture of bovine preantral follicles and assess whether
372 bESCs could be differentiated towards progenitor cells of the bipotential gonad using
373 stepwise in vitro culture protocols. The ultimate goal of this work is to develop novel
374 assisted reproductive technologies that enable the use of small preantral follicles in
375 conjunction with renewable theca-like cells for oocyte production. Since maintaining
376 structural integrity of the follicle is a main concern with 2D culture, hydrogels represent a
377 viable option as they provide framework to maintain the 3D configuration of follicles while
378 permitting growth. Indeed, the theory to build a culture system complete with extracellular

379 matrix components like the ovary has been suggested when early studies first explored
380 bovine preantral in vitro development [27]. Further adaptations to include sophisticated
381 ECM components in the hydrogel design have permitted mouse follicle growth in vitro
382 starting as early as the primordial stage [28]. Our finding that ECM-degrading enzymes
383 such as MMPs, PLAT and PLAU are expressed by bovine preantral follicles agrees with
384 previous investigations in follicles and spent medium [37,38]. However, the fact that these
385 transcripts were not uniformly expressed in all pools examined could indicate an intrinsic
386 variability in the ability of the follicles to remodel the ECM. This could explain at least in
387 part the variability observed in growth rate in the present study. Although we found that
388 PEG hydrogels outperformed 2D control over 10 days in primary follicles, there was a
389 notable difference in the percentage of follicles that grew between replicates (each
390 represented by one ovary), further underlining the biological variability between samples
391 and possibly an inherent propensity of some follicles for growth versus atresia. A limitation
392 of this study using slaughterhouse-derived oocytes is the inability to track factors known
393 to affect follicle viability such as animal age, nutritional and health status. Of note, early
394 secondary follicles showed a stagnant rate of growth compared to primary follicles
395 cultured in PEG hydrogels; this stagnation suggests that either 1) the 10 day-culture
396 conditions remain substandard for bovine preantral follicles or 2) follicles canonically slow
397 their growth at this stage of development which is a phenomenon seen in mice [29]. It is
398 worth noting that in vivo, 10 days represents a very narrow window within the estimated
399 180 days of folliculogenesis in the cow, and therefore relatively small changes in growth
400 could be expected in normally-developing follicles.

We tested the hypothesis of enhancing the bovine follicle culture system with cellular supplementation as others have shown that the addition of ovarian stromal cells, fibroblasts, and adipose-derived stem cells promote survival and growth of preantral follicles in several species [13,17–19,30]. When BOCs were encapsulated in PEG hydrogels and cultured, we found cell aggregates which may be due to absence of basement membrane binding proteins in the PEG composition, rendering the cells unable to adhere to the matrix and resulting in self-aggregation. Indeed, cell-extracellular matrix interactions are important for mediating complex cellular responses such as migration, proliferation, and differentiation [31], thus BOCs were likely incapable of integrating well throughout the hydrogel. Furthermore, the finding of decreased expression of genes known to be important for the pre-theca cell phenotype after culture shows that the BOCs did not maintain their identity, which could have contributed to the lack of success of this 3D co-culture system. Others have reported that mouse ovarian stromal cells transition from a predominately theca-like identity to almost entirely macrophage identity after 12 days of in vitro culture with follicles, partially corroborating our findings of theca cell loss [32]. Since we found similarly high signs of atresia between follicles co-encapsulated and follicles in PEG-only hydrogels, we pose the possibility that the prolonged protocol required to dissociate ovarian tissue, isolate and label follicles, and process for encapsulation may have contribute to decrease follicle viability beginning at day 0. In future experiments, pre-theca cells could be sorted (pending availability of reliable antibodies against specific theca cell surface markers) before incorporation into the PEG hydrogel. Furthermore, culture conditions that specifically support theca cell phenotype would likely need to be investigated.

424 In an attempt to produce gonadal-like cells for supplementation as pre-theca-like
425 cells in follicle culture, we employed bovine embryonic stem cells to recapitulate
426 mesoderm formation and early differentiation of the bipotential gonad with defined media
427 conditions. We show that inclusion of exogenous signaling factors such as the GSK3β
428 inhibitor CHIR 99021 for activation of WNT. WNT signaling can drive bESCs into
429 intermediate mesoderm-like cells that show early signs of coelomic epithelial-like
430 phenotype as indicated by gene and protein expression. During embryonic development,
431 the sexually dimorphic gonad (ovary or testis) must develop beginning from the
432 mesoderm germ layer, and then further differentiate into the intermediate mesoderm, then
433 coelomic epithelium which ingresses and gives rise to the sexually amorphic "bipotential
434 gonad" [33,34]. More specifically, upon Nodal, WNT and FGF signaling to induce
435 mesoderm differentiation [35], a subset of cells in the caudal aspect of the early
436 gastrulated embryo are specified to become precursors of the bipotential gonad.
437 Signaling by WNT, Nodal, and FGF during anterior-posterior (A-P) body axis extension,
438 which occurs at peri-gastrulation and is regulated by TBXT and other morphogens in the
439 mesoderm, drives cell fate decisions that result in caudal body axis formation [36,37].
440 Concomitantly, mediolateral segmentation occurs when a low, medium, and high gradient
441 of BMP signaling drives mesoderm cells into the paraxial, intermediate, and lateral plate
442 mesoderm domains, respectively [38,39]. Following this knowledge of developmental
443 biology, we chose to modulate WNT, Nodal, FGF and BMP signaling to mimic the
444 molecular events that drive cell differentiation for pre-gonad development during early
445 embryogenesis as shown in several mammalian species [34]. However, through these
446 experiments, we found that under WNT activation, bFGF and BMP4 are not essential to

447 induce the intermediate mesoderm or early coelomic epithelium. We observed peak
448 expression of the intermediate mesoderm marker *LHX1* after 48 h of mesoderm induction
449 under WNT and activin A, the latter a known inducer of *Lim1* (i.e. *Lhx1*) that has an
450 important role in IM specification/kidney development [40]. We also found *OSR1*
451 upregulated in all conditions after MeLC induction. *OSR1* is an early marker of IM and
452 others have shown its necessity for the urogenital phenotype [41–43] and generating
453 somatic cells of the gonad from PSCs [44]. Thus, we propose these cells may be reaching
454 the IM state with possible capability of becoming progenitor bipotential gonad-like.
455 Nevertheless, *OSR1* is not exclusive of the IM or gonads; kidney progenitor and lateral
456 plate mesoderm cells express *OSR1* [43,45] and this marker is used to demarcate kidney
457 progenitor-like cells during in vitro differentiation of PSCs [46–48]. Therefore, our
458 intermediate mesoderm/early coelomic epithelium-like cells should be further evaluated
459 for markers of early nephrogenesis.

460 We additionally found a rise in *WT1,* which is also an early, and more restrictive,
461 marker of gonadal progenitor cells [49], in induced cells across all bFGF and BMP4
462 regimens compared to bESCs. This indicates that continuous WNT activation for 3
463 additional days after initial mesoderm induction can provoke *WT1* expression. WT1 is
464 found along the A-P axis of mice as early as E9.0, with overlapping expression of GATA4
465 and NR5A1 in the coelomic epithelium by E10.0 and onward [49]. Moreover, WT1
466 activates the NR5A1 promoter [50], thus driving early gonad development. Interestingly,
467 *WT1* upregulation was accompanied by *GATA4* upregulation when 10 or 20 ng/mL of
468 BMP4 was included in culture which aligns with other studies [51]. However, we found
469 variable expression of the protein WT1 in cells cultured beyond MeLC induction and after

470 3 additional days under 0 or 1 ng/mL of BMP4. Although typically found in the nucleus,
471 WT1 isoforms with capability of shuttling between the nucleus and cytoplasm, therefore
472 we postulate various WT1 isoforms with nuclear and/or cytoplasmic activity may be
473 expressed in our cells [52]. We additionally highlight that there was no difference in *PAX3*
474 in all experiments, demonstrating that our culture conditions did not favor differentiation
475 of the paraxial mesoderm lineage. Interestingly, increasing BMP4 concentrations led to
476 increased expression of *FOXF1* (lateral plate mesoderm marker), which aligns with in
477 vivo studies showing a higher gradient of BMPs specifies the lateral plate of developing
478 embryos [39].

479 Our findings provide seminal context to previous work looking at differentiation of
480 ESCs from humans and mouse to gonad-like cells by using combinations of BMP4, FGF,
481 CHIR, and activin A [53–55]. Alternative approaches to inducing gonad-like cell formation
482 include overexpression of key transcription factors such as *SF1*, *WT1*, *RUNX1*, and
483 *GATA4* [56,57]. The efficiency of induction can be variable when using small molecules
484 or genetic engineering for differentiating stem cells, therefore heterogeneity in cell identity
485 would be expected in the present study. Although not done in this study, cell-sorting based
486 on expression of key markers could aid in purifying cell populations of interest and used
487 for downstream in vitro culture to achieve bipotential and even ovary or testis- like cells.
488 Yet, in vivo early somatic progenitor cells of the bipotential gonad are not specified
489 homogeneously, therefore some heterogeneity could be warranted, especially when
490 forming organoids as self-organizing structures. Finally, future studies should examine
491 early bovine embryonic development in vivo as findings from these studies could shed

light on the species-specific molecular mechanisms that drive gonad formation and inform future in vitro culture conditions to recapitulate the process.

In conclusion, these findings provide a key step in expanding current understanding of in vitro preantral folliculogenesis using a non-rodent model as well as sheds light on methodologies in differentiating bESCs into precursor-like cells of the ovary. The convergence of these two technologies will be pivotal to broadening the knowledge base of follicle development and early gonadogenesis such that novel assisted reproductive technologies can be expanded.

ACKNOWLEDGEMENTS

The authors acknowledge Stephanie McDonnell and Amanda Morton for aiding in follicle collection and isolation. Funding: NIH 1F31HD111173, UC Davis Jastro Shields Graduate Research Award, and Gary B. Anderson Food Animal Fellowship to JC; USDA-NIFA W4112, 4171 multi-state groups.

AUTHOR CONTRIBUTION

Conceptualization: Juliana Candelaria, Anna Denicol; Methodology: Juliana Candelaria, Carly Guiltinan, Ramon Botigelli, Ariella Shikanov, Anna Denicol; Formal analysis and investigation: Juliana Candelaria, Anna Denicol; Writing - original draft preparation: Juliana Candelaria; Writing - review and editing: Juliana Candelaria, Anna Denicol, Ariella Shikanov, Carly Guiltinan, Ramon Botigelli,; Funding acquisition: Juliana Candelaria, Anna Denicol; Resources: Anna Denicol, Ariella Shikanov; Supervision: Anna Denicol.

COMPETING INTERESTS

The authors declare no competing interests.

REFERENCES

1. Bus A, Langbeen A, Martin B, Leroy JLMR, Bols PEJ. Is the pre-antral ovarian follicle the 'holy grail'for female fertility preservation? Anim Reprod Sci [Internet]. 2019;207:119–30. Available from: http://www.sciencedirect.com/science/article/pii/S0378432019302064

2. Gutierrez CG, Ralph JH, Telfer EE, Wilmut I, Webb R. Growth and Antrum Formation of Bovine Preantral Follicles in Long-Term Culture In Vitro1. Biol Reprod [Internet]. 2000;62:1322–8. Available from: https://doi.org/10.1095/biolreprod62.5.1322

3. Araújo VR, Gastal MO, Wischral A, Figueiredo JR, Gastal EL. Long-term in vitro culture of bovine preantral follicles: Effect of base medium and medium replacement methods. Anim Reprod Sci [Internet]. 2015;161:23–31. Available from: http://www.sciencedirect.com/science/article/pii/S0378432015001736

4. Rossetto R, Saraiva MVA, Bernuci MP, Silva GM, Brito IR, Alves A, et al. Impact of insulin concentration and mode of FSH addition on the in vitro survival and development of isolated bovine preantral follicles. Theriogenology [Internet]. 2016/05/22. 2016;86:1137–45. Available from: https://www.ncbi.nlm.nih.gov/pubmed/27207475

5. Gomes JE, Correia SC, Gouveia-Oliveira A, Cidadão AJ, Plancha CE. Three-dimensional environments preserve extracellular matrix compartments of ovarian follicles and increase FSH-dependent growth. Mol Reprod Dev. 1999;54:163–72.

6. Belli M, Vigone G, Merico V, Redi CA, Zuccotti M, Garagna S. Towards a 3D culture of mouse ovarian follicles. International Journal of Developmental Biology. 2013;56:931–7.

7. Xu M, West-Farrell ER, Stouffer RL, Shea LD, Woodruff TK, Zelinski MB. Encapsulated Three-Dimensional Culture Supports Development of Nonhuman Primate Secondary Follicles1. Biol Reprod. 2009;81:587–94.

8. Xu J, Lawson MS, Yeoman RR, Molskness TA, Ting AY, Stouffer RL, et al. Fibrin promotes development and function of macaque primary follicles during encapsulated three-dimensional culture. Hum Reprod [Internet]. 2013/04/21. 2013;28:2187–200. Available from: https://pubmed.ncbi.nlm.nih.gov/23608357

9. Vanacker J, Luyckx V, Dolmans MM, Des Rieux A, Jaeger J, Van Langendonckt A, et al. Transplantation of an alginate–matrigel matrix containing isolated ovarian cells: First step in developing a biodegradable scaffold to transplant isolated preantral follicles and ovarian cells. Biomaterials. 2012;33:6079–85.

10. Ihm JE, Lee ST, Han DK, Lim JM, Hubbell JA. Murine ovarian follicle culture in PEG-hydrogel: Effects of mechanical properties and the hormones FSH and LH on development. Macromol Res [Internet]. 2015;23:377–86. Available from: https://doi.org/10.1007/s13233-015-3045-x

11. Mendez U, Zhou H, Shikanov A. Synthetic PEG Hydrogel for Engineering the Environment of Ovarian Follicles. In: Chawla K, editor. Methods in Molecular Biology [Internet]. New York, NY: Springer New York; 2018. p. 115–28. Available from: https://doi.org/10.1007/978-1-4939-7741-3_9

12. Shikanov A, Smith RM, Xu M, Woodruff TK, Shea LD. Hydrogel network design using multifunctional macromers to coordinate tissue maturation in ovarian follicle culture.

558 Biomaterials [Internet]. 2011;32:2524–31. Available from:
559 http://dx.doi.org/10.1016/j.biomaterials.2010.12.027

560 13. Tomaszewski CE, Constance E, Lemke MM, Zhou H, Padmanabhan V, Arnold KB, et
561 al. Adipose-derived stem cell-secreted factors promote early stage follicle development
562 in a biomimetic matrix. Biomater Sci. 2019;7:571–80.

563 14. Wijgerde M, Ooms M, Hoogerbrugge JW, Grootegoed JA. Hedgehog signaling in
564 mouse ovary: Indian hedgehog and desert hedgehog from granulosa cells induce target
565 gene expression in developing theca cells. Endocrinology. 2005;146:3558–66.

566 15. Cowan RG, Quirk SM. Cells responding to hedgehog signaling contribute to the theca
567 of ovarian follicles. Reproduction. 2021;161:437–48.

568 16. Russell MC, Cowan RG, Harman RM, Walker AL, Quirk SM. The hedgehog signaling
569 pathway in the mouse ovary. Biol Reprod. 2007;77:226–36.

570 17. Grubliauskaitė M, Vlieghe H, Moghassemi S, Dadashzadeh A, Camboni A,
571 Gudlevičienė Ž, et al. Influence of ovarian stromal cells on human ovarian follicle growth
572 in a 3D environment. Hum Reprod Open. 2023;2023.

573 18. Tingen CM, Kiesewetter SE, Jozefik J, Thomas C, Tagler D, Shea L, et al. A
574 macrophage and theca cell-enriched stromal cell population influences growth and
575 survival of immature murine follicles in vitro. Reproduction. 2011;141:809–20.

576 19. Tagler D, Tu T, Smith RM, Anderson NR, Tingen CM, Woodruff TK, et al. Embryonic
577 Fibroblasts Enable the Culture of Primary Ovarian Follicles Within Alginate Hydrogels.
578 Tissue Eng Part A [Internet]. 2012;18:1229–38. Available from:
579 https://doi.org/10.1089/ten.tea.2011.0418

580 20. Jadhav U, Jameson JL. Steroidogenic factor-1 (SF-1)-driven differentiation of murine
581 embryonic stem (ES) cells into a gonadal lineage. Endocrinology. 2011;152:2870–82.

582 21. Lan C-W, Chen M-J, Jan P-S, Chen H-F, Ho H-N. Differentiation of Human Embryonic
583 Stem Cells Into Functional Ovarian Granulosa-like Cells. J Clin Endocrinol Metab
584 [Internet]. 2013;98:3713–23. Available from: https://doi.org/10.1210/jc.2012-4302

585 22. Rodríguez Gutiérrez D, Eid W, Biason-Lauber A. A Human Gonadal Cell Model From
586 Induced Pluripotent Stem Cells. Front Genet [Internet]. 2018;9. Available from:
587 https://www.frontiersin.org/articles/10.3389/fgene.2018.00498

588 23. Knarston IM, Pachernegg S, Robevska G, Ghobrial I, Er PX, Georges E, et al. An In
589 Vitro Differentiation Protocol for Human Embryonic Bipotential Gonad and Testis Cell
590 Development. Stem Cell Reports [Internet]. 2020;15:1377–91. Available from:
591 https://doi.org/10.1016/j.stemcr.2020.10.009

592 24. Sepponen K, Lundin K, Knuus K, Väyrynen P, Raivio T, Tapanainen JS, et al. The role
593 of sequential BMP signaling in directing human embryonic stem cells to bipotential
594 gonadal cells. Journal of Clinical Endocrinology and Metabolism. 2017;102:4303–14.

595 25. Danti L, Lundin K, Sepponen K, Yohannes DA, Kere J, Tuuri T, et al. CRISPR/Cas9-
596 mediated activation of NR5A1 steers female human embryonic stem cell-derived
597 bipotential gonadal-like cells towards a steroidogenic cell fate. J Ovarian Res [Internet].
598 2023;16:194. Available from: https://doi.org/10.1186/s13048-023-01264-5

599 26. McDonnell SP, Candelaria JI, Morton AJ, Denicol AC. Isolation of Small Preantral
600 Follicles from the Bovine Ovary Using a Combination of Fragmentation, Homogenization,
601 and Serial Filtration. JoVE [Internet]. 2022; Available from: https://www.jove.com/64423

602 27. Figueiredo JR de, Hulshof SCJ, Thiry M, Van Den Hurk R, Bevers MM, Nusgens B,
603 et al. Extracellular matrix proteins and basement membrane: Their identification in bovine
604 ovaries and significance for the attachment of cultured preantral follicles. Theriogenology.
605 1995;43:845–58.

606 28. Nason-Tomaszewski CE, Thomas EE, Matera DL, Baker BM, Shikanov A.
607 Extracellular matrix-templating fibrous hydrogels promote ovarian tissue remodeling and
608 oocyte growth. Bioact Mater [Internet]. 2024;32:292–303. Available from:
609 https://doi.org/10.1016/j.bioactmat.2023.10.001

610 29. Richard S, Anderson NJ, Zhou Y, Pankhurst MW. Mouse primary follicles experience
611 slow growth rates after activation and progressive increases that influence the duration
612 of the primary follicle phase. Biol Reprod. 2023;109:684–92.

613 30. Green LJ, Zhou H, Padmanabhan V, Shikanov A. Adipose-derived stem cells promote
614 survival, growth, and maturation of early-stage murine follicles. Stem Cell Res Ther.
615 2019;10:1–13.

616 31. Hynes RO. Stretching the boundaries of extracellular matrix research. Nat Rev Mol
617 Cell Biol [Internet]. 2014;15:761–3. Available from: https://doi.org/10.1038/nrm3908

618 32. Tingen CM, Kiesewetter SE, Jozefik J, Thomas C, Tagler D, Shea L, et al. A
619 macrophage and theca cell-enriched stromal cell population influences growth and
620 survival of immature murine follicles in vitro. Reproduction [Internet]. 2011/03/09.
621 2011;141:809–20. Available from: https://pubmed.ncbi.nlm.nih.gov/21389078

622 33. Karl J, Capel B. Sertoli cells of the mouse testis originate from the coelomic
623 epithelium. Dev Biol. 1998;203:323–33.

624 34. Rotgers E, Jørgensen A, Yao HHC. At the crossroads of fate-Somatic cell lineage
625 specification in the fetal gonad. Endocr Rev. 2018;39:739–59.

626 35. Ciruna B, Rossant J. FGF signaling regulates mesoderm cell fate specification and
627 morphogenetic movement at the primitive streak. Dev Cell. 2001;1:37–49.

628 36. Amin S, Neijts R, Simmini S, van Rooijen C, Tan SC, Kester L, et al. Cdx and T
629 Brachyury Co-activate Growth Signaling in the Embryonic Axial Progenitor Niche. Cell
630 Rep [Internet]. 2016;17:3165–77. Available from:
631 https://doi.org/10.1016/j.celrep.2016.11.069

632 37. Brennan J, Lu CC, Norris DP, Rodriguez TA, Beddington RSP, Robertson EJ. Nodal
633 signalling in the epiblast patterns the early mouse embryo. Nature. 2001;411:965–9.

634 38. James RG, Schultheiss TM. Bmp signaling promotes intermediate mesoderm gene
635 expression in a dose-dependent, cell-autonomous and translation-dependent manner.
636 Dev Biol. 2005;288:113–25.

637 39. Niehrs C, Dosch R, Onichtchouk D. Embryonic patterning of Xenopus mesoderm by
638 Bmp-4. Of Fish, Fly, Worm, and Man: Lessons from Developmental Biology for Human
639 Gene Function and Disease. 2000;165–90.

640 40. Preger-Ben Noon E, Barak H, Guttmann-Raviv N, Reshef R. Interplay between activin
641 and Hox genes determines the formation of the kidney morphogenetic field. Development
642 [Internet]. 2009;136:1995–2004. Available from: https://doi.org/10.1242/dev.035592

643 41. Wang Q, Lan Y, Cho ES, Maltby KM, Jiang R. Odd-skipped related 1 (Odd1) is an
644 essential regulator of heart and urogenital development. Dev Biol. 2005;288:582–94.

645 42. Mae S-I, Shono A, Shiota F, Yasuno T, Kajiwara M, Gotoda-Nishimura N, et al.
646 Monitoring and robust induction of nephrogenic intermediate mesoderm from human
647 pluripotent stem cells. Nat Commun [Internet]. 2013;4:1367. Available from:
648 https://doi.org/10.1038/ncomms2378

649 43. James RG, Kamei CN, Wang Q, Jiang R, Schultheiss TM. Odd-skipped related 1 is
650 required for development of the metanephric kidney and regulates formation and
651 differentiation of kidney precursor cells. Development. 2006;133:2995–3004.

652 44. Yoshino T, Suzuki T, Nagamatsu G, Yabukami H, Ikegaya M, Kishima M, et al.
653 Generation of ovarian follicles from mouse pluripotent stem cells. Science (1979).
654 2021;373.

655 45. Xu J, Liu H, Park J-S, Lan Y, Jiang R. Osr1 acts downstream of and interacts
656 synergistically with Six2 to maintain nephron progenitor cells during kidney
657 organogenesis. Development [Internet]. 2014;141:1442–52. Available from:
658 https://doi.org/10.1242/dev.103283

659 46. Araoka T, Mae S, Kurose Y, Uesugi M, Ohta A, Yamanaka S, et al. Efficient and Rapid
660 Induction of Human iPSCs/ESCs into Nephrogenic Intermediate Mesoderm Using Small
661 Molecule-Based Differentiation Methods. PLoS One [Internet]. 2014;9:e84881. Available
662 from: https://doi.org/10.1371/journal.pone.0084881

663 47. Morizane R, Lam AQ, Freedman BS, Kishi S, Valerius MT, Bonventre J V. Nephron
664 organoids derived from human pluripotent stem cells model kidney development and
665 injury. Nat Biotechnol [Internet]. 2015;33:1193–200. Available from:
666 https://doi.org/10.1038/nbt.3392

667 48. Takasato M, Er PX, Becroft M, Vanslambrouck JM, Stanley EG, Elefanty AG, et al.
668 Directing human embryonic stem cell differentiation towards a renal lineage generates a
669 self-organizing kidney. Nat Cell Biol [Internet]. 2014;16:118–26. Available from:
670 https://doi.org/10.1038/ncb2894

671 49. Sasaki K, Oguchi A, Cheng K, Murakawa Y, Okamoto I, Ohta H, et al. The embryonic
672 ontogeny of the gonadal somatic cells in mice and monkeys. Cell Rep [Internet].
673 2021;35:109075. Available from: https://doi.org/10.1016/j.celrep.2021.109075

674 50. Wilhelm D, Englert C. The Wilms tumor suppressor WT1 regulates early gonad
675 development by activation of Sf1. Genes Dev. 2002;16:1839–51.

676 51. Rojas A, De Val S, Heidt AB, Xu S-M, Bristow J, Black BL. Gata4 expression in lateral
677 mesoderm is downstream of BMP4 and is activated directly by Forkhead and GATA
678 transcription factors through a distal enhancer element. Development [Internet].
679 2005;132:3405–17. Available from: https://doi.org/10.1242/dev.01913

52. Niksic M, Slight J, Sanford JR, Caceres JF, Hastie ND. The Wilms' tumour protein (WT1) shuttles between nucleus and cytoplasm and is present in functional polysomes. Hum Mol Genet [Internet]. 2004;13:463–71. Available from: https://doi.org/10.1093/hmg/ddh040

53. Gonen N, Eozenou C, Mitter R, Elzaiat M, Stévant I, Aviram R, et al. In vitro cellular reprogramming to model gonad development and its disorders. Sci Adv. 2023;9.

54. Rore H, Owen N, Piña-Aguilar RE, Docherty K, Sekido R. Testicular somatic cell-like cells derived from embryonic stem cells induce differentiation of epiblasts into germ cells. Commun Biol [Internet]. 2021;4. Available from: http://dx.doi.org/10.1038/s42003-021-02322-8

55. Shin E-Y, Park S, Choi WY, Lee DR. Rapid Differentiation of Human Embryonic Stem Cells into Testosterone-Producing Leydig Cell-Like Cells In vitro. Tissue Eng Regen Med [Internet]. 2021;18:651–62. Available from: https://doi.org/10.1007/s13770-021-00359-8

56. Xu C, Mohsin A, Luo Y, Xie L, Peng Y, Wang Q, et al. Differentiation roadmap of embryonic Sertoli cells derived from mouse embryonic stem cells. Stem Cell Res Ther. 2019;10:1–12.

57. Smela MDP, Kramme CC, Fortuna PRJ, Adams JL, Su R, Dong E, et al. Directed differentiation of human iPSCs to functional ovarian granulosa-like cells via transcription factor overexpression. Elife. 2023;12.

701 **Table 1** Primer list.

Gene	Forward Sequence (5'-3')	Reverse Sequence (5'-3')	Product size (base pairs)
BAX	CATGAGGTCAACCCTCGGGA	TAG GGA AGC CCA TGCTGAGT	117
BCL2	GAGTTCGGAGGGGTCATGTG	GGG CCA TAC AGC TCCACAAA	158
CSPG4	CTGGAGGAACAA AGGTCTCTGG	ACTGCGTGATCTGGAAAAGCA	140
DHH	GCATGCATTGCAGGTCGTC	ACGTGGGCAGAATGCTAGTC	145
FOXF1	GCCTCCTACATCAAGCAGCA	GTTCTGGTGCAGATACGGCT	108
GATA4	TGCGCCCCATCAAAACAGAG	GGGCCATACAGCTCCACAAA	77
GLI1	CCTTCAAAGCCCAGTACATGC	GTGCGTCTTCAGATTTTCCAG	122
IHH	CGGCTTCGACTGGGTGTATT	GGCTGAGTGCTCGGACTTG	70
LHX1	TGGACCGCTTCCTCTTGAAC	CTTGGTACCGAAACACCGGA	152
MMP2	ATCGTCTTCGACGGC ATCTC	TTCGCCAGATGAATCGGTCC	70
MMP9	CTTCACCTTTGAGGGTCGCT	TGGGTGTAGAGTCTCTCGCT	138
OSR1	CCTGTGGAAATCCAGCGCC	CAGTCTGTTCTGACTTCCTGCTTA	111
PAX3	CCTTCAAAGCCCAGTACATGC	GTGCGTCTTCAGATTTTCCAG	122
PLAT	TCGGCAGGCCCTCTATTCTT	ACGTGGCGGTAGCATCTATTT	89
PLAU	TGGGTCAGTCACGGCTTAAC	ACGGATCTTCAGCAAGGCAAT	131
WT1	CCTTCACCGTCCACTTCTCT	CCGTGCTGTATCCCTGGTTG	183
H2A.2	GAGGAGCTGAACAAGCTGTTG	TTGTGGTGGCTCTCAGTCTTC	104
ACTB	CTCTTCCAGCCTTCCTTCCT	GGGCAGTGATCTCTTTCTGC	178

702
703

A

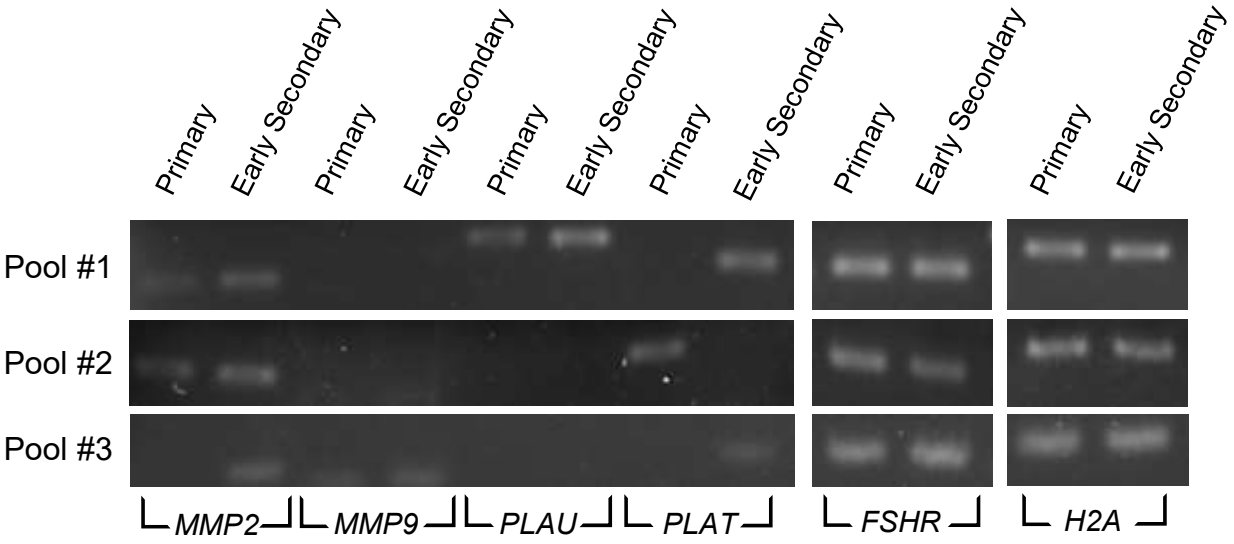
Primary
Early Secondary
Primary
Early Secondary
Primary
Early Secondary
Primary
Early Secondary
Primary
Early Secondary
Primary
Early Secondary
Pool #1
Pool #2
Pool #3
MMP2
MMP9
PLAU
PLAT
FSHR
H2A

B

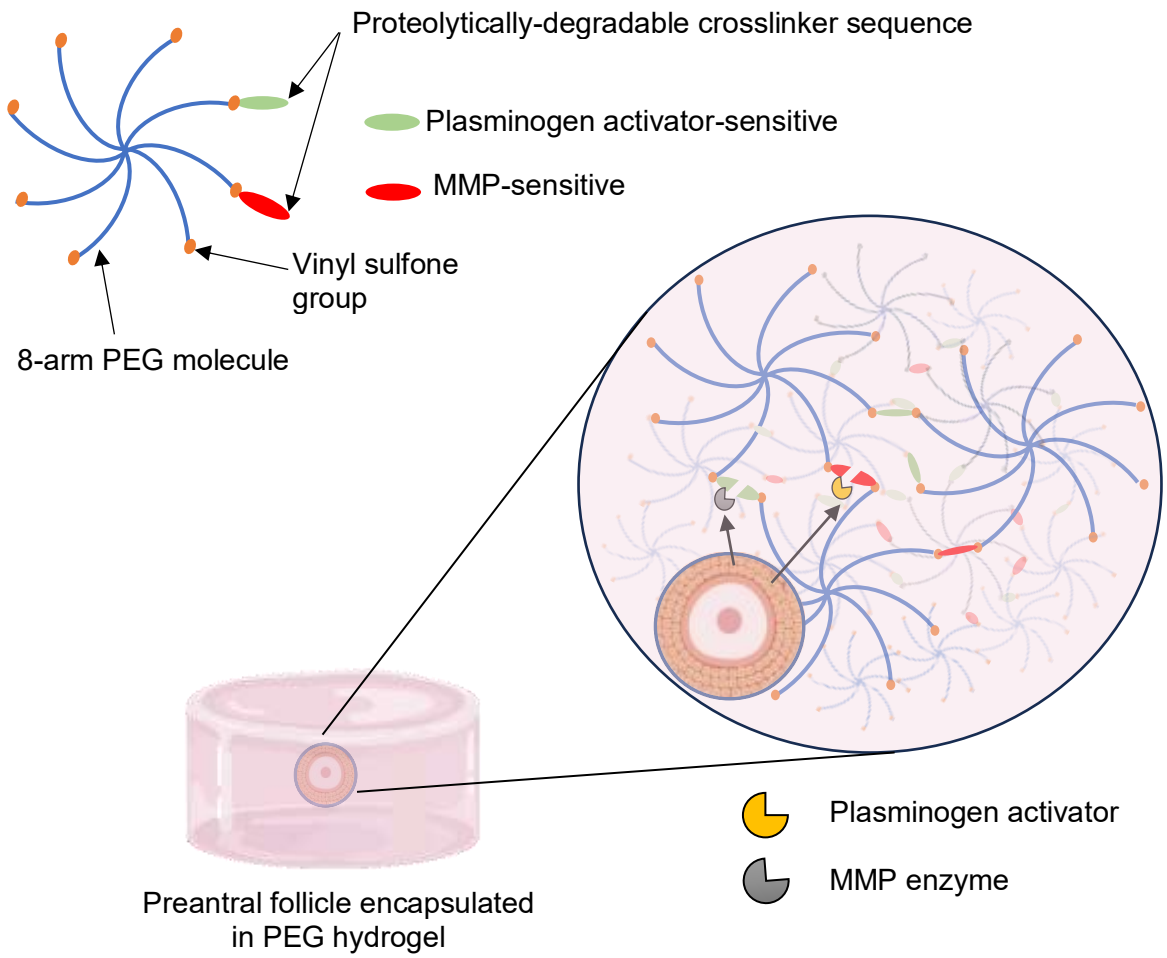
Proteolytically-degradable crosslinker sequence
Plasminogen activator-sensitive
MMP-sensitive
Vinyl sulfone group
8-arm PEG molecule
Plasminogen activator
MMP enzyme
Preantral follicle encapsulated in PEG hydrogel

Fig 1 Bovine preantral follicles express extracellular matrix-degrading enzymes, allowing the design of a PEG hydrogel containing target peptides for controlled degradation. (**A**) Agarose gel with products of RT-PCR of primary and early secondary follicles expressing mRNA for *MMP2, MMP9, PLAU, PLAT, FSHR,* and *H2A.* Each pool of primary and early secondary follicles (n = 3 pools per stage) contained 46-56 and 34-40 follicles, respectively. (**B**) Schematic of PEG hydrogel for follicle encapsulation. PEG = poly(ethylene glycol). MMP = matrix metalloproteinase

758

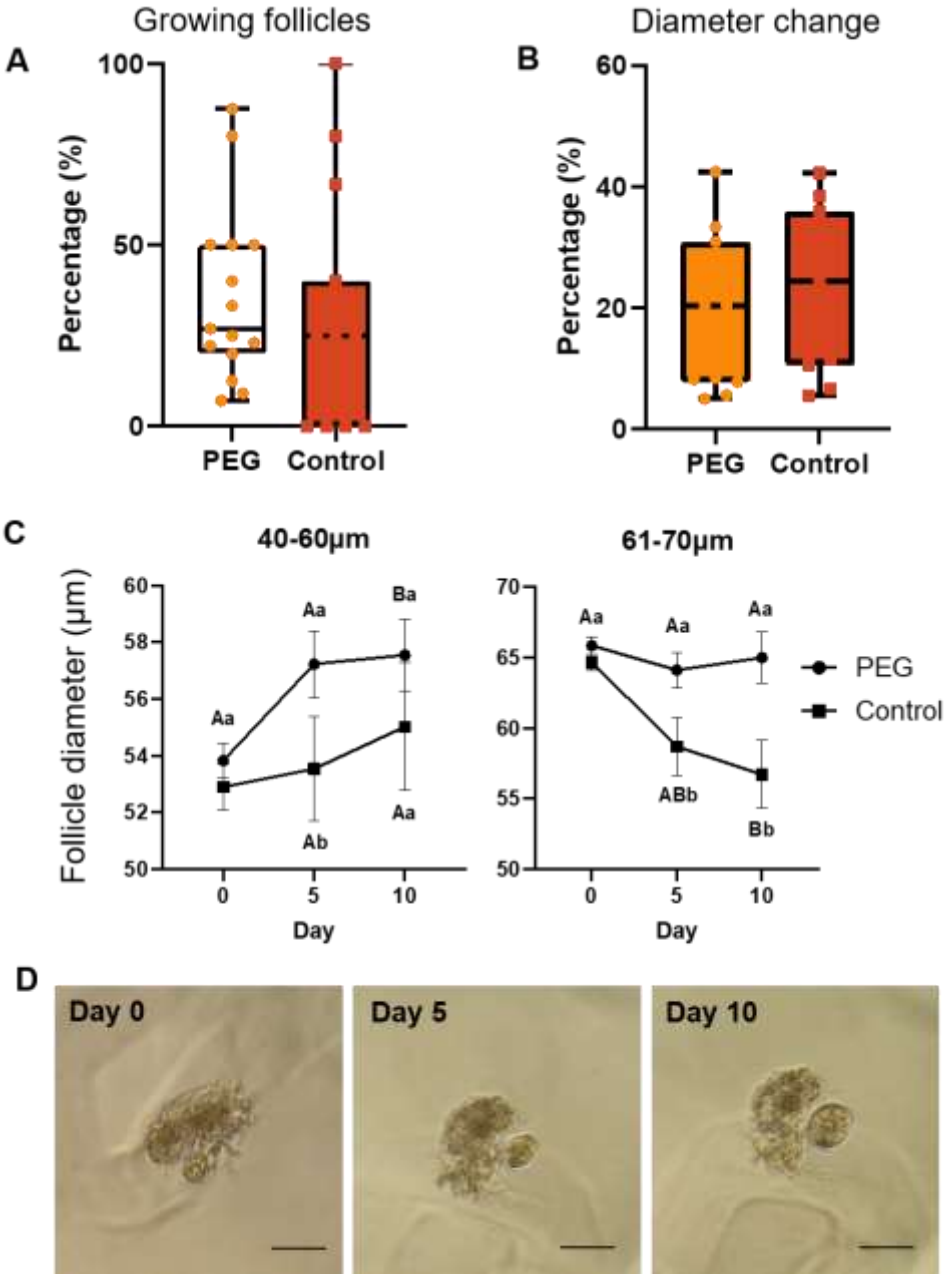

759

760 **Fig 2** Bovine preantral follicle in vitro growth using PEG or 2D control culture systems.
761 Percentage of preantral follicles that grew (**A**) and percent change in diameter from
762 follicles that grew (**B**). (**C**) Bovine preantral follicle diameter growth during in vitro culture
763 at indicated starting diameters/stages. Lowercases letters that differ = significant
764 difference ($P < 0.05$) between treatment groups in the same day. Uppercase letters that
765 differ = significant difference ($P < 0.05$) within the same treatment group but compared to
766 day 0. Data are presented as mean ± SEM. (**D**) Representative images of follicle grown
767 in PEG over 10-day culture period. Scale bar = 100 µm.

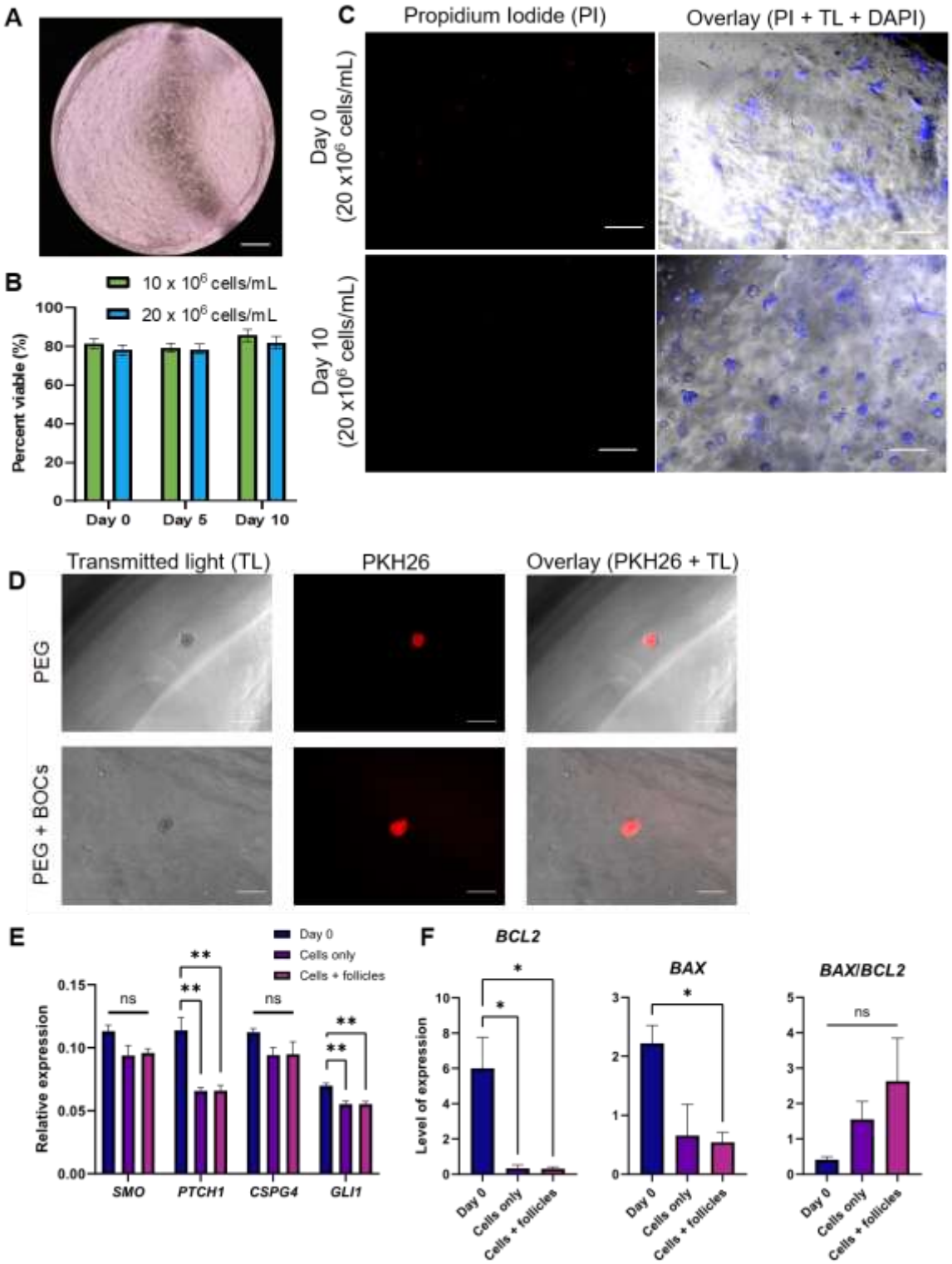

Fig 3 Co-culture of bovine preantral follicles with bovine ovarian cells (BOCs) in PEG hydrogels. (**A**) Representative image of BOCs in PEG hydrogel (scale bar = 500 µm). (**B**) Viability of BOCs encapsulated in PEG hydrogels during in vitro culture. (**C**) Propidium iodine (PI) staining in BOCs encapsulated in PEG hydrogels at day 0 and day 10 of

773 culture. Counterstained with DAPI (TL = transluminescent; scale bar = 100 μm). (**D**)
774 Unviable preantral follicle encapsulated in PEG hydrogel with or without BOCs using
775 PKH26 to label follicles at day 10 of culture (scale bar = 100 μm). (**E**) Gene expression of
776 pre-theca cell markers in BOCs (relative expression = 1/ΔCT). (**F**) Anti- and pro-apoptotic
777 gene marker expression in BOCs (level of expression = absolute quantification from
778 standard curve). Data are presented as mean ± SEM.
779

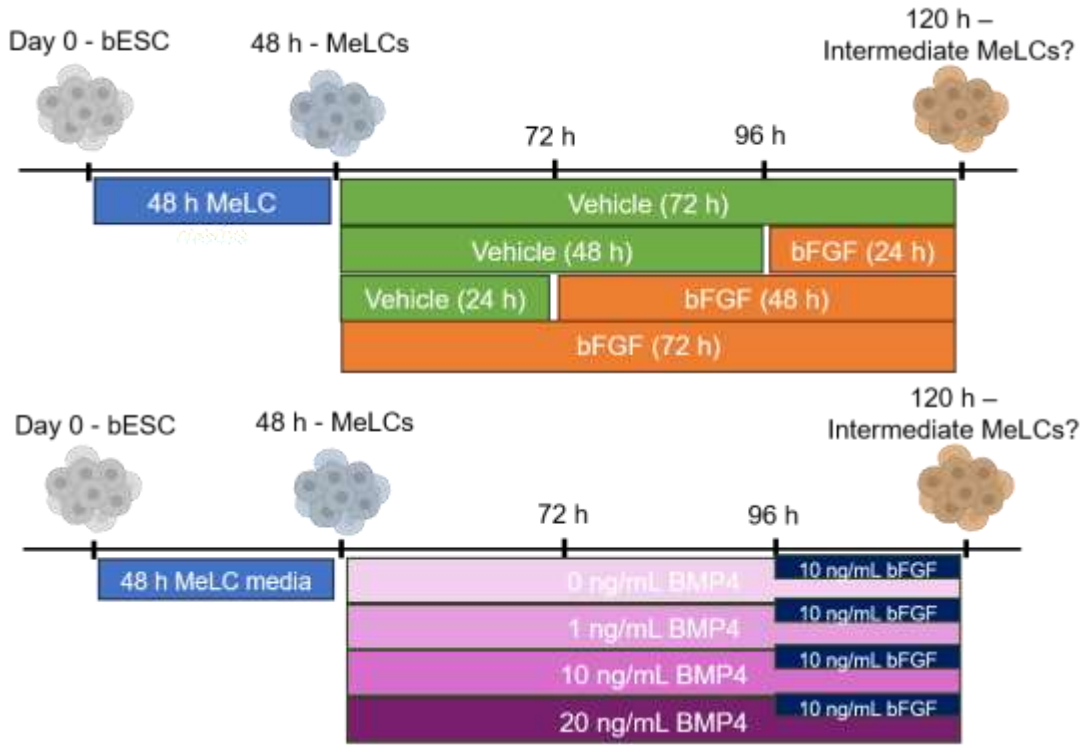
Day 0 - bESC
48 h - MeLCs
120 h –
Intermediate MeLCs?
72 h
96 h
48 h MeLC
Vehicle (72 h)
Vehicle (48 h)
bFGF (24 h)
Vehicle (24 h)
bFGF (48 h)
bFGF (72 h)
Day 0 - bESC
48 h - MeLCs
120 h –
Intermediate MeLCs?
72 h
96 h
48 h MeLC media
0 ng/mL BMP4
1 ng/mL BMP4
10 ng/mL BMP4
20 ng/mL BMP4
10 ng/mL bFGF
10 ng/mL bFGF
10 ng/mL bFGF
10 ng/mL bFGF

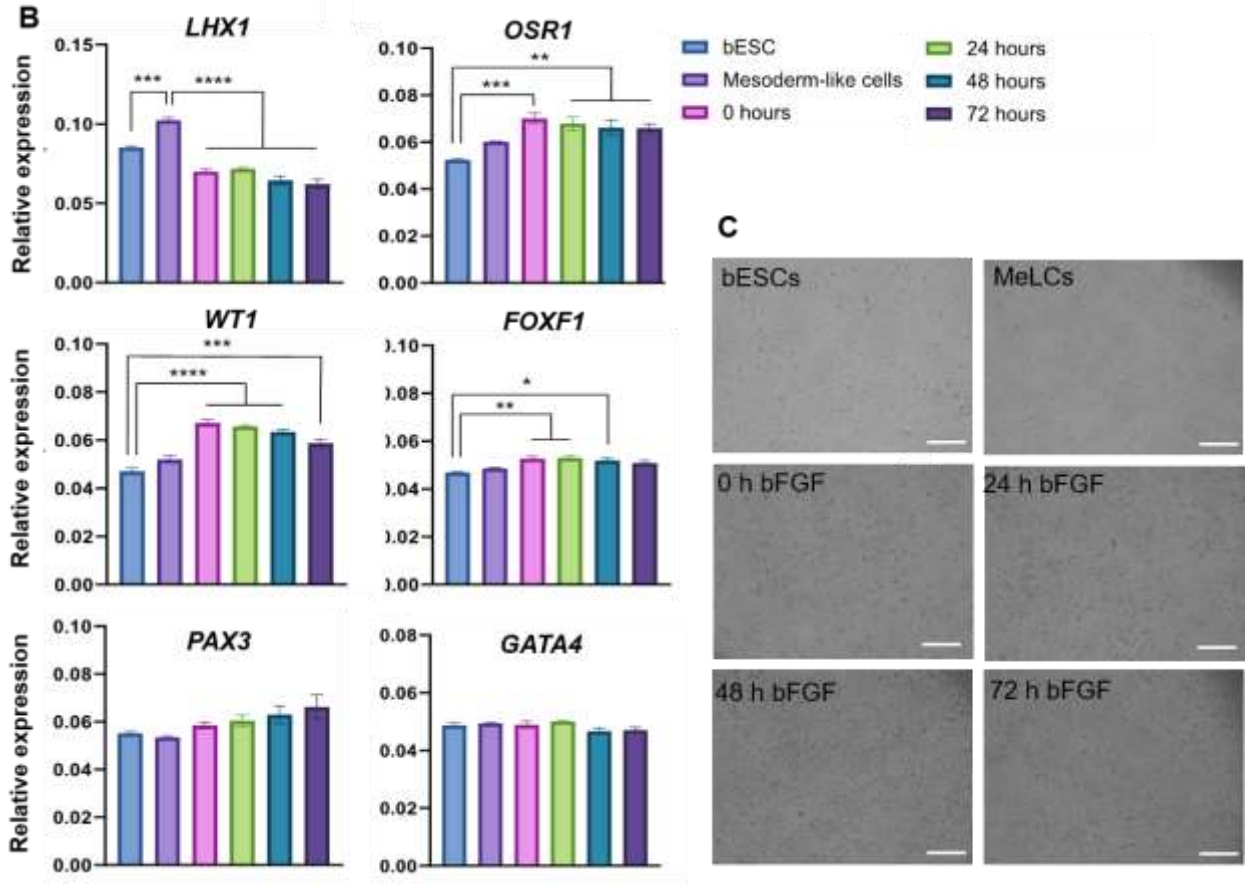
B
LHX1
OSR1
WT1
FOXF1
PAX3
GATA4
Relative expression
bESC
Mesoderm-like cells
0 hours
24 hours
48 hours
72 hours
C
bESCs
MeLCs
0 h bFGF
24 h bFGF
48 h bFGF
72 h bFGF

783
784 **Fig 4** In vitro differentiation of bovine embryonic stem cells (bESCs) towards progenitors
785 of somatic bipotential gonad-like cells. (**A**) Schematic diagram of experimental design for
786 bFGF and BMP4 experiments. (**B**) Gene expression of intermediate mesoderm,
787 bipotential gonad, paraxial and lateral plate mesoderm markers before and after bESC
788 differentiation using bFGF at various days of exposure. (**C**) Representative images of
789 cells from each treatment group. Data are presented as mean ± SEM. Significant
790 differences are noted by * = P <0.05, ** = P <0.01, *** = P <0.001, **** = P <0.0001.
791

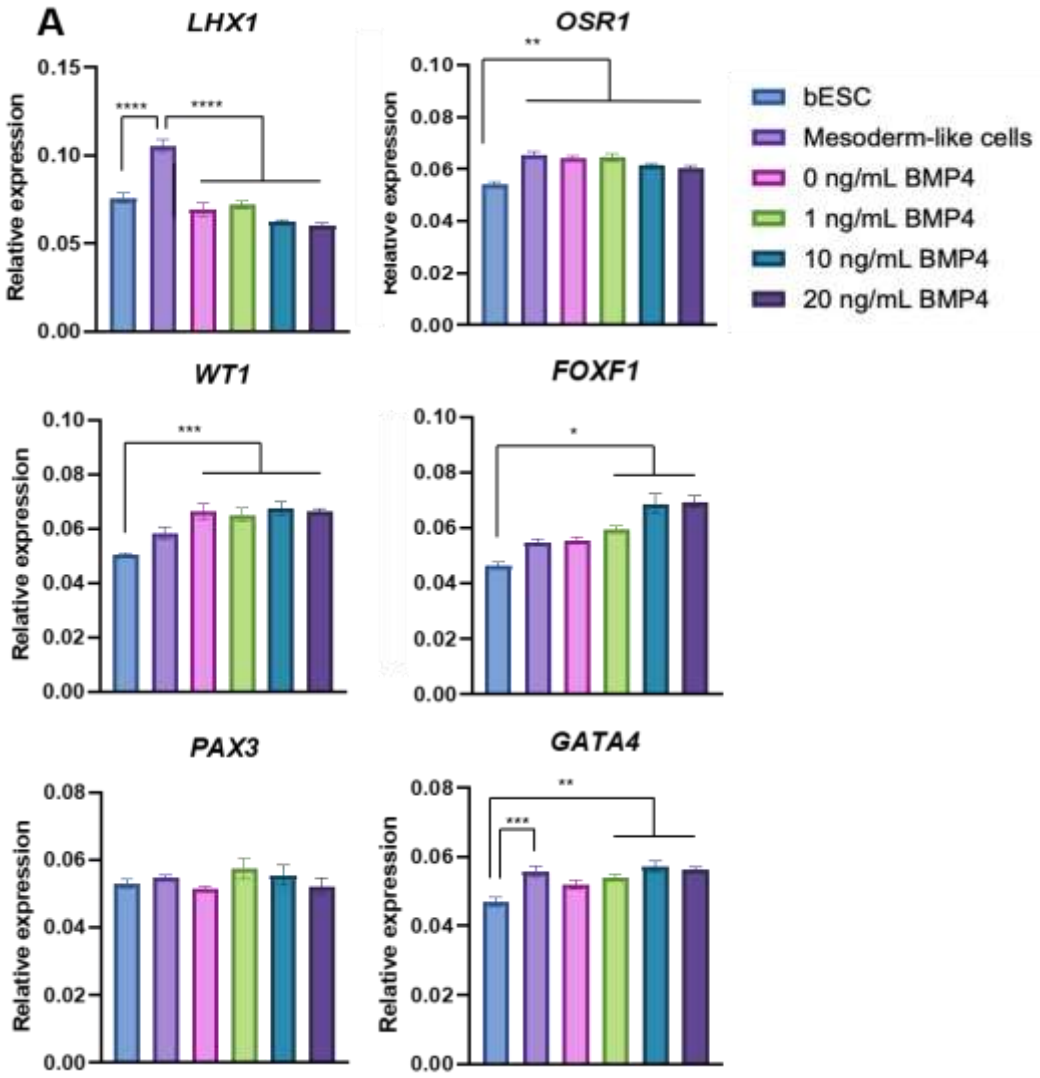
A
LHX1
OSR1
WT1
FOXF1
PAX3
GATA4
Relative expression
bESC
Mesoderm-like cells
0 ng/mL BMP4
1 ng/mL BMP4
10 ng/mL BMP4
20 ng/mL BMP4

792

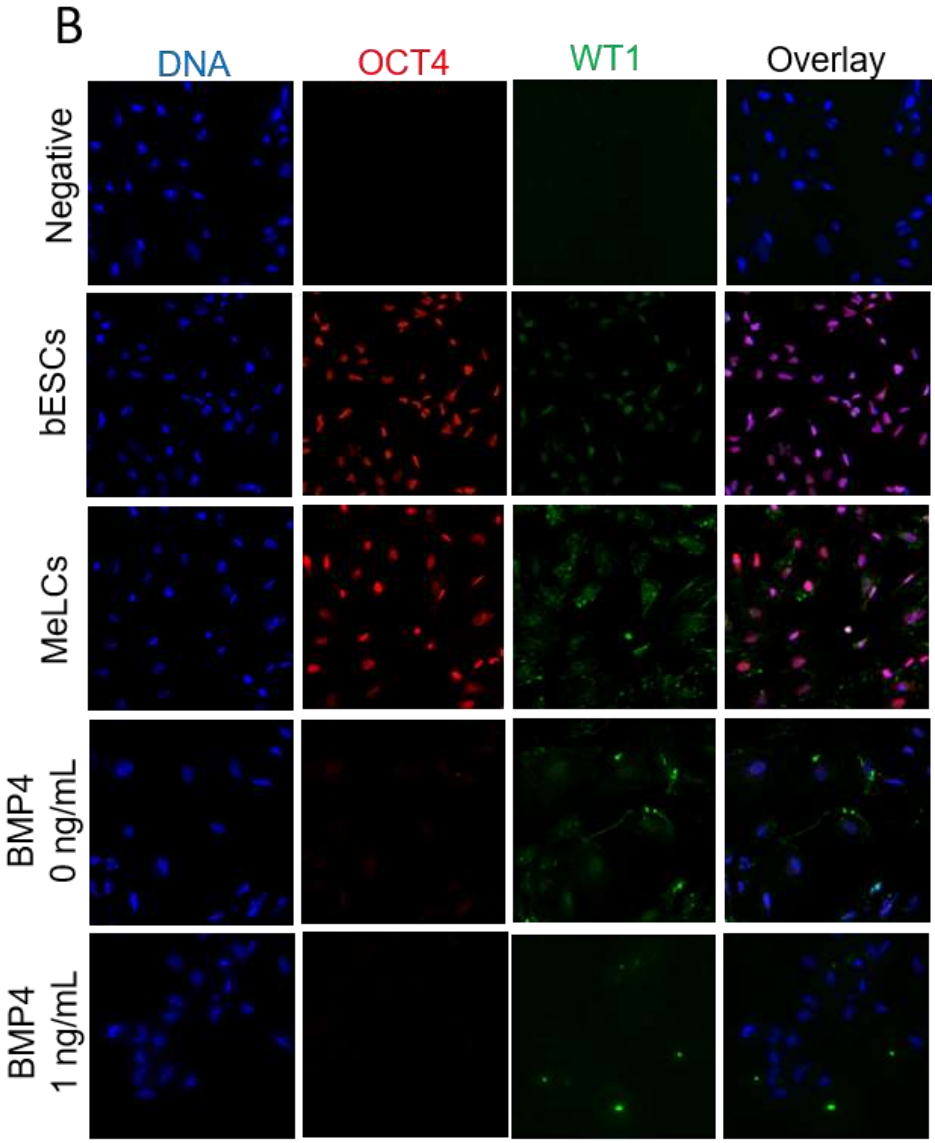

Fig 5 In vitro differentiation of bovine embryonic stem cells (bESCs) towards progenitors of somatic bipotential gonad-like cells testing BMP4 concentrations. (**A**) Gene expression of intermediate mesoderm, bipotential gonad, paraxial and lateral plate mesoderm markers before and after bESC differentiation (**B**) Representative images of cells from each treatment group. Data are presented as mean ± SEM. Significant differences are noted by * = P <0.05, ** = P <0.01, *** = P <0.001, **** = P <0.0001.